



**HAL**  
open science

# Biot-JKD model: simulation of 1D transient poroelastic waves

Emilie Blanc, Guillaume Chiavassa, Bruno Lombard

► **To cite this version:**

Emilie Blanc, Guillaume Chiavassa, Bruno Lombard. Biot-JKD model: simulation of 1D transient poroelastic waves. Acoustics 2012, Apr 2012, Nantes, France. hal-00810599

**HAL Id: hal-00810599**

**<https://hal.science/hal-00810599>**

Submitted on 23 Apr 2012

**HAL** is a multi-disciplinary open access archive for the deposit and dissemination of scientific research documents, whether they are published or not. The documents may come from teaching and research institutions in France or abroad, or from public or private research centers.

L'archive ouverte pluridisciplinaire **HAL**, est destinée au dépôt et à la diffusion de documents scientifiques de niveau recherche, publiés ou non, émanant des établissements d'enseignement et de recherche français ou étrangers, des laboratoires publics ou privés.



# ACOUSTICS 2012

## Biot-JKD model: simulation of 1D transient poroelastic waves

E. Blanc<sup>a</sup>, G. Chiavassa<sup>b</sup> and B. Lombard<sup>a</sup>

<sup>a</sup>Laboratoire de Mécanique et d'Acoustique, 31, Chemin Joseph Aiguier - 13402 Marseille  
Cedex 20

<sup>b</sup>Ecole Centrale Marseille, 38 rue Joliot Curie, 13451 Marseille, France  
eblanc@lma.cnrs-mrs.fr

This article deals with time-domain numerical modeling of Biot poroelastic waves. The viscous dissipation inside the pores is described by the model of dynamic permeability of Johnson-Koplik-Dashen (JKD). Some coefficients of the Biot-JKD model are proportional to the square root of the frequency. In the time-domain, they introduce shifted fractional derivatives of order  $1/2$ , which involves a convolution product. A diffusive representation replaces the convolution kernel by a finite number of memory variables that satisfy local-in-time ordinary differential equations. Based on the dispersion relation, the coefficients of the diffusive representation are determined by optimization on the frequency range of interest. A numerical modeling based on a splitting strategy is proposed: the propagative part is discretized by a fourth-order ADER scheme on a Cartesian grid, whereas the diffusive part is solved exactly. Comparisons with analytical solutions are proposed, demonstrating the efficiency and the accuracy of the approach.

## 1 Introduction

The propagation of waves in porous media has crucial implications in many areas in applied mechanics, such as the characterization of industrial foams, spongy bones and petroleum rocks. We consider the 1D Biot-JKD model, which describes the viscous dissipation in the high-frequency range (HF) in the case of pores of random geometry. This model involves a frequency correction  $\widehat{F}(\omega)$ , depending on the square root of the frequency. In the time-domain, shifted fractional derivatives are introduced, which requires to store the past values of the solution. Computational effort is therefore largely increased, and large simulations are out of reach. Our aim is to propose a much more efficient approach.

To do so, we use a diffusive approximation of the fractional derivatives. The fractional derivatives are then replaced by a finite number  $N$  of diffusive variables, that satisfy local-in-time differential equations. The coefficients of the approximation are determined by least-squares optimization on the frequency range of interest, depending on the spectrum of the source. The number  $N$  of diffusive variables can be estimated in terms of the required accuracy. The whole system of the evolution equations is then integrated using a splitting method: the propagative part is solved with a temporally and spatially fourth-order accurate ADER scheme, and the diffusive part is solved exactly. Numerical experiments of wave propagation are proposed; they show both the quality of the diffusive approximation and the accuracy of the numerical integration.

## 2 Physical modeling

### 2.1 Biot-JKD model

The Biot-JKD model describes the propagation of mechanical waves in a porous medium and accounts for the viscous dissipation in the high-frequency range. It is assumed that [1, 2, 3]:

- the wavelengths are large compared with the diameter of the pores;
- the amplitudes of perturbations are small;
- the elastic and isotropic matrix is fully saturated by a single fluid phase;
- the thermomechanical effects are neglected.

This model relies on 11 physical parameters: the density  $\rho_f$  and the dynamic viscosity  $\eta$  of the fluid; the density  $\rho_s$  and the shear modulus  $\mu$  of the elastic skeleton; the porosity  $0 < \phi < 1$ , the tortuosity  $a \geq 1$ , the absolute permeability  $\kappa$ ,

the Lamé coefficient  $\lambda_f$ , the two Biot coefficients  $\beta$  and  $m$  of the saturated matrix and the viscous characteristic length  $\Lambda$ . The following notations are introduced:  $\rho_w = \frac{a}{\phi} \rho_f$ ,  $\rho = \phi \rho_f + (1 - \phi) \rho_s$ ,  $\chi = \rho \rho_w - \rho_f^2 > 0$ ,  $\lambda_0 = \lambda_f - m \beta^2$ ,  $C = \lambda_0 + 2\mu > 0$ . Using a velocity-stress formulation, the unknowns in 1D are the elastic velocity  $v_s = \frac{\partial u_s}{\partial t}$ , the filtration velocity  $w = \frac{\partial W}{\partial t} = \phi(v_f - v_s)$  where  $v_f = \frac{\partial u_f}{\partial t}$  is the fluid velocity, the elastic stress  $\sigma$ , and the acoustic pressure  $p$ . In one hand, the constitutive laws are:

$$\begin{cases} \sigma = (\lambda_f + 2\mu) \varepsilon - m \beta \xi, \\ p = m(-\beta \varepsilon + \xi), \end{cases} \quad (1)$$

where  $\varepsilon = \frac{\partial u_s}{\partial x}$  is the strain tensor and  $\xi = -\frac{\partial W}{\partial x}$  is the rate of fluid change. On the other hand, the conservation of momentum yields:

$$\begin{cases} \rho \frac{\partial v_s}{\partial t} + \rho_f \frac{\partial w}{\partial t} = \frac{\partial \sigma}{\partial x}, \\ \rho_s \frac{\partial v_s}{\partial t} + \rho_w \frac{\partial w}{\partial t} + \frac{\eta}{\kappa} F * w = -\frac{\partial p}{\partial x}, \end{cases} \quad (2)$$

where  $*$  is the convolution product in time. The second equation of (2) is the generalized Darcy's law. Using the Fourier transform  $\mathcal{F}(F(t)) = \widehat{F}(\omega) = \int_{\mathbb{R}} F(t) e^{-i\omega t} dt$  and introducing the notations

$$f_c = \frac{\omega_c}{2\pi} = \frac{\eta \phi}{2\pi a \kappa \rho_f}, \quad P = \frac{4a\kappa}{\phi \Lambda^2}, \quad \Omega = \frac{\omega_c}{P} = \frac{\eta \phi^2 \Lambda^2}{4a^2 \kappa^2 \rho_f}, \quad (3)$$

the frequency correction of the Biot-JKD model [3] is:

$$\begin{aligned} \widehat{F}_{JKD}(\omega) &= \left( 1 + i\omega \frac{4a^2 \kappa^2 \rho_f}{\eta \Lambda^2 \phi^2} \right)^{1/2}, \\ &= \left( 1 + iP \frac{\omega}{\omega_c} \right)^{1/2}, \\ &= \frac{1}{\sqrt{\Omega}} (\Omega + i\omega)^{1/2}. \end{aligned} \quad (4)$$

Setting  $D_{\Omega} w(x, t) = \frac{\partial w}{\partial t} + \Omega w$ , the term  $F * w$  in (2) is therefore written:

$$\begin{aligned} F_{JKD}(t) * w(x, t) &= \mathcal{F}^{-1} \left( \frac{1}{\sqrt{\Omega}} (\Omega + i\omega)^{1/2} \widehat{w}(x, \omega) \right), \\ &= \frac{1}{\sqrt{\Omega}} (D + \Omega)^{1/2} w(x, t), \\ &= \frac{1}{\sqrt{\pi}} \int_0^t \frac{e^{-\Omega(t-\tau)}}{\sqrt{t-\tau}} D_{\Omega} w(x, \tau) d\tau. \end{aligned} \quad (5)$$

The operator  $(D + \Omega)^{1/2}$  is a shifted fractional derivative of order 1/2 [8, 9]. It generalizes the classical derivative characterized by  $\frac{\partial w}{\partial t} = \mathcal{F}^{-1}(i\omega \widehat{w})$ .

Using (1), (2) and (5), the Biot-JKD equations lead to a first-order non-homogeneous linear system of partial differential equations:

$$\begin{cases} \frac{\partial v_s}{\partial t} - \frac{\rho_w}{\chi} \frac{\partial \sigma}{\partial x} - \frac{\rho_f}{\chi} \frac{\partial p}{\partial x} = \frac{\rho_f}{\rho} \gamma (D + \Omega)^{1/2} w, \\ \frac{\partial w}{\partial t} + \frac{\rho_f}{\chi} \frac{\partial \sigma}{\partial x} + \frac{\rho}{\chi} \frac{\partial p}{\partial x} = -\gamma (D + \Omega)^{1/2} w, \\ \frac{\partial \sigma}{\partial t} - (\lambda_f + 2\mu) \frac{\partial v_s}{\partial x} - m\beta \frac{\partial w}{\partial x} = 0, \\ \frac{\partial p}{\partial t} + m\beta \frac{\partial v_s}{\partial x} + m \frac{\partial w}{\partial x} = 0, \end{cases} \quad (6)$$

where  $\gamma = \frac{\eta}{\kappa} \frac{\rho}{\chi} \frac{1}{\sqrt{\Omega}}$ .

## 2.2 Diffusive representation

The operator  $(D + \Omega)^{1/2}$  in (5) is not local-in-time, contrary to classical derivatives. A straightforward discretization of (6) therefore requires to store the past values of  $w$ , which highly penalizes the numerical modeling and prevents from studying large configurations. Injecting a diffusive representation of the decreasing function  $\frac{1}{\sqrt{t}}$

$$\frac{1}{\sqrt{t}} = \int_0^\infty \frac{1}{\sqrt{\pi}} \frac{1}{\sqrt{\theta}} e^{-\theta t} d\theta, \quad (7)$$

in (5), we obtain:

$$\begin{aligned} (D + \Omega)^{1/2} w(x, t) &= \frac{1}{\pi} \int_0^t \int_0^\infty \frac{e^{-(\theta + \Omega)(t - \tau)}}{\sqrt{\theta}} D_\Omega w(x, \tau) d\theta d\tau, \\ &= \frac{1}{\pi} \int_0^\infty \frac{1}{\sqrt{\theta}} \psi(x, t, \theta) d\theta. \end{aligned} \quad (8)$$

For the sake of clarity, we omit the dependence on  $\Omega$  and  $w$  in the diffusive variable

$$\psi(x, t, \theta) = \int_0^t e^{-(\theta + \Omega)(t - \tau)} D_\Omega w(x, \tau) d\tau, \quad (9)$$

From (9),  $\psi$  satisfies the following differential equation:

$$\begin{cases} \frac{\partial \psi}{\partial t} = -(\theta + \Omega)\psi + D_\Omega w, \\ \psi(x, 0, \theta) = 0. \end{cases} \quad (10)$$

The diffusive representation transforms a non local-in-time problem (5) in a continuum (8) of local-in-time problems (10). We note that the diffusive representation just modifies the writing of the fractional derivative and does not introduce any approximation. Lastly, the diffusive representation enables to prove the well-posedness of Biot-JKD model, as stated in the following proposition.

**Proposition 1** *Let*

$$E = E_1 + E_2 + E_3,$$

with

$$E_1 = \frac{1}{2} \int_{\mathbb{R}} (\rho v^2 + \rho_w w^2 + 2\rho_f v w) dx,$$

$$E_2 = \frac{1}{2} \int_{\mathbb{R}} \left( \frac{1}{C} (\sigma + \beta p)^2 + \frac{1}{m} p^2 \right) dx,$$

$$E_3 = \frac{1}{2} \int_{x \in \mathbb{R}} \int_{\theta \in \mathbb{R}^+} \frac{\eta}{\kappa} \frac{1}{\pi} \frac{1}{\sqrt{\Omega \theta}} \frac{1}{\theta + 2\Omega} (w - \psi)^2 d\theta dx. \quad (11)$$

Then  $E \geq 0$  is the mechanical energy of the Biot-JKD system, and it satisfies

$$\frac{dE}{dt} = - \int_{x \in \mathbb{R}} \int_{\theta \in \mathbb{R}^+} \frac{\eta}{\kappa} \frac{1}{\pi} \frac{\Omega w^2 + (\theta + \Omega) \psi^2}{\sqrt{\Omega \theta} (\theta + 2\Omega)} d\theta dx \leq 0. \quad (12)$$

## 3 Diffusive approximation: Biot-AD model

We use a quadrature rule on  $N$  points to approximate the integral in (8). Let  $(a_\ell, \theta_\ell)$  be the weights and the abscissas of this diffusive approximation (AD):

$$\begin{aligned} (D + \Omega)^{1/2} w(x, t) &\simeq \sum_{\ell=1}^N a_\ell \psi(x, t, \theta_\ell), \\ &= \sum_{\ell=1}^N a_\ell \psi_\ell(x, t). \end{aligned} \quad (13)$$

We replace the fractional derivatives in (6) by their diffusive approximation (13). Doing so, we obtain a new mathematical model, called Biot-AD, well-suited for time-domain numerical modeling. After some calculations, we get:

$$\frac{\partial \mathbf{U}}{\partial t} + \mathbf{A} \frac{\partial \mathbf{U}}{\partial x} = -\mathbf{S} \mathbf{U}, \quad (14)$$

where  $\mathbf{U} = (v_s, w, \sigma, p, \psi_1, \dots, \psi_N)^T$ , and  $\mathbf{A}$ ,  $\mathbf{S}$  are  $(N + 4)^2$  matrices. The size of the problem to solve increases with the number  $N$  of diffusive variables, and thus with the quality of the diffusive approximation of the fractional derivatives. Depending on the model, Biot-JKD or Biot-AD, the frequency correction in the second equation of (2) can be written:

$$\widehat{F}(\omega) = \begin{cases} \widehat{F}_{JKD}(\omega) = \frac{1}{\sqrt{\Omega}} (\Omega + i\omega)^{1/2}, \\ \widehat{F}_{AD}(\omega) = \frac{\Omega + i\omega}{\sqrt{\Omega}} \sum_{\ell=1}^N \frac{a_\ell}{\theta_\ell + \Omega + i\omega}. \end{cases} \quad (15)$$

Now, we determine the coefficients of the diffusive representation  $a_\ell$  and  $\theta_\ell$  in (13). To do so,  $\widehat{F}_{JKD}(\omega)$  is approximated by  $\widehat{F}_{AD}(\omega)$  (15) over  $[\omega_{min}, \omega_{max}]$  depending on the central frequency of the source  $f_0 = \frac{\omega_0}{2\pi}$ . We choose  $\omega_{min} = \omega_0/10$  et  $\omega_{max} = 10\omega_0$ . The coefficients  $a_\ell$  and  $\theta_\ell$  are obtained by a classical linear least-squares optimization procedure in the  $L_2$  norm [11, 12]. The relaxation angular frequencies are distributed linearly on a logarithmic scale of  $N$  points:

$$\theta_\ell = \omega_{min} \left( \frac{\omega_{max}}{\omega_{min}} \right)^{\frac{\ell-1}{N-1}}, \quad \ell = 1, \dots, N. \quad (16)$$

The weights  $a_\ell$  are then obtained by minimizing the  $L_2$  norm of

$$(\Omega + i\tilde{\omega}_k)^{1/2} \sum_{\ell=1}^N \frac{1}{\theta_\ell + \Omega + i\omega_k} a_\ell - 1, \quad k = 1, \dots, N, \quad (17)$$

where  $\tilde{\omega}_k$  are distributed linearly on a logarithmic scale of  $N$  points:

$$\tilde{\omega}_k = \omega_{\min} \left( \frac{\omega_{\max}}{\omega_{\min}} \right)^{\frac{k-1}{N-1}}, \quad k = 1, \dots, N. \quad (18)$$

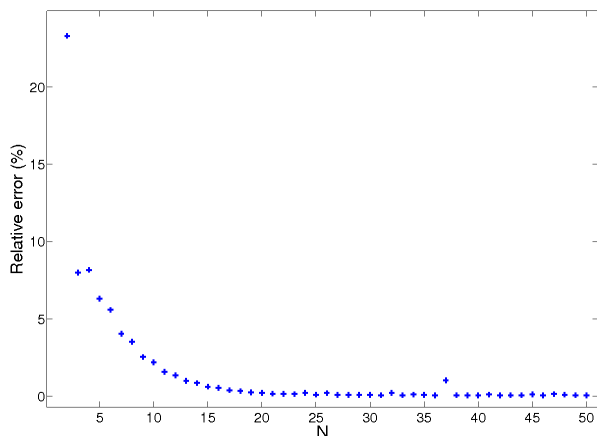


Figure 1: Approximation of the Biot-JKD model by the Biot-AD model. Relative error of model  $\varepsilon_m$  versus the number of diffusive variables  $N$ .

Now, we determine the number  $N$  of diffusive variables in terms of both the chosen accuracy  $\varepsilon_m$  and the ratio  $f_0/f_c$ . As a criterion of error, we use the relative error in  $L_2$  norm between  $\widehat{F}_{AD}(\omega)$  and  $\widehat{F}_{JKD}(\omega)$  (figure 1), which amounts to the energy of error of model. In figure 1, we note that  $N = 6$  is required to obtain  $\varepsilon_m \leq 2.5\%$ . A parametric determination of  $N$  in terms of  $\varepsilon_m$  and  $f_0/f_c$  is proposed in figure 2. The observed stairs-steps are due to the fact that  $N$  is an integer. To get more accurate results, we observe that  $N$  must be logically increased.

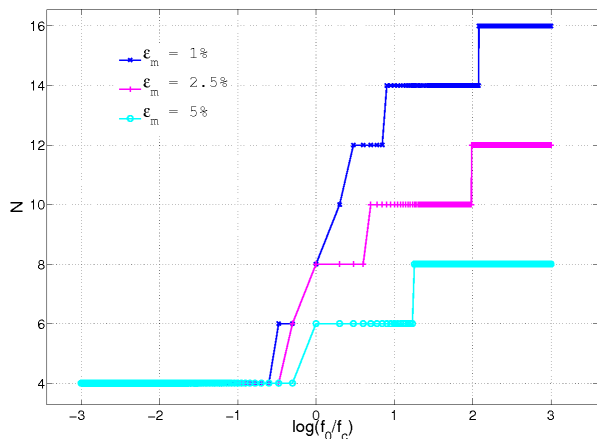


Figure 2: Number of diffusive variables  $N$  versus  $f_0/f_c$  and the accuracy of model  $\varepsilon_m$ .

## 4 Numerical modeling

To integrate the system (14), we consider a uniform grid, with the spatial mesh size  $\Delta x$  and the time step  $\Delta t$ . An approximation  $U_j^n$  of  $U(x_j = j\Delta x, t_n = n\Delta t)$  is sought. We solve alternatively the propagative part (first equation of (19)) and the diffusive part (second equation of (19)) by Strang's splitting:

$$\begin{cases} \frac{\partial U}{\partial t} + A \frac{\partial U}{\partial x} = 0, \\ \frac{\partial U}{\partial t} = -S U. \end{cases} \quad (19)$$

The propagative part is solved using a temporally and spatially fourth-order accurate ADER scheme, and the diffusive part is solved exactly. The integration (19) yields the optimal CFL stability condition:

$$\text{CFL} = C_{pf}^\infty \frac{\Delta t}{\Delta x} \leq 1, \quad (20)$$

where  $C_{pf}^\infty$  is the high-frequency limit of the phase velocity of the fast wave. The diffusive part is unconditionally stable. Since  $A$  and  $S$  do not commute, the theoretical order of convergence in time and in space falls from 4 to 2. Using the ADER 4 scheme is nevertheless advantageous, compared with the second-order accurate ADER scheme (Lax-Wendroff): numerical artifacts, such as dispersion and attenuation, are greatly reduced.

## 5 Numerical experiments

### 5.1 Parameters

We consider sandstone saturated with water (medium  $\Omega_0$  in [6]). The frequency of transition is  $f_c \approx 3845$  Hz. The source is a Dirac in space:  $h(x) = \delta(x - x_0)$ , where  $x_0 = 0$  m. The temporal evolution of the source  $g(t)$  is a  $C^6$  truncated sinusoid with a central frequency  $f_0 = 200$  kHz ( $f_0/f_c \approx 50$ ). The point source symmetrically generates left-going waves and right-going waves. Fast and slow waves are denoted by  $P_f$  and  $P_s$ . The JKD frequency correction mainly affects the slow waves; all the observations are therefore made on these waves.

The computational domain studied  $[-0.04, 0.04]$  m is discretized on a mesh of  $N_x = 700$  points (32 points per slow wavelength and 104 points per fast wavelength). The time step follows from (20) with  $\text{CFL} = 0.9$ . Errors are measured in  $L_2$  norm on the domain  $[0, 0.007]$  m, centered on the right-going slow wave at  $t_1 \approx 8.63 \cdot 10^{-6}$  s. The analytical solutions of Biot-JKD and Biot-AD are obtained by Fourier synthesis: we use the band of frequencies  $[0, 62.5 f_0]$ , and the number of Fourier modes is  $N_f = 9.6 \cdot 10^5$  ( $\Delta f \approx 13$  Hz). We choose  $N = 6$  diffusive variables. The numerical experiments are performed on a processor Intel Core i7 (2.80 GHz).

### 5.2 Test 1: numerical validation of Biot-AD

The aim of this test is to validate the numerical modeling of the approximate Biot-AD system. The figure 3 shows the numerical Biot-AD (circle) and analytical Biot-AD (solid line) values of the pressure, after 200 iterations ( $t_1 \approx 8.63 \cdot 10^{-6}$  s). We note the excellent agreement between these two curves. More quantitatively, the relative error measured is  $\varepsilon_n \approx 1.70\%$ .

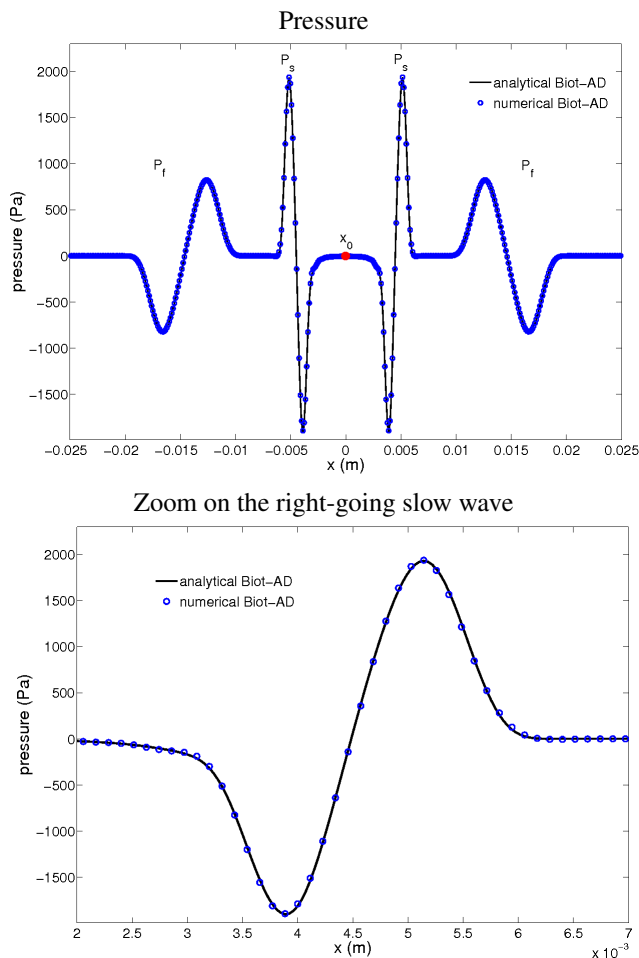


Figure 3: Test 1. Fast waves  $P_f$  and slow waves  $P_s$  generated by a point source centered on  $x_0 = 0$  m. Comparison between the numerical Biot-AD (circle) and analytical Biot-AD (solid line) values of the pressure at  $t_1 \approx 8.63 \cdot 10^{-6}$  s.

Next, we measure the numerical error  $\varepsilon_n$  for several  $N_x$ . The values of the measured error and the local convergence rates are given in table 1. The figure 4 shows  $\varepsilon_n$  versus  $1/N_x$ , using a logarithmic scale. The convergence rate measured by linear regression is 1.990, close to the second order theoretically predicted.

Table 1: Test 1. Measure of the convergence rate.

$N_x$	Error $L_2$	Convergence rate
1000	$2.235 \cdot 10^{-1}$	-
2000	$1.571 \cdot 10^{-2}$	3.853
3000	$4.176 \cdot 10^{-3}$	3.353
4000	$2.047 \cdot 10^{-3}$	2.558
5000	$1.273 \cdot 10^{-3}$	2.166
6000	$8.817 \cdot 10^{-4}$	2.032
7000	$6.494 \cdot 10^{-4}$	1.989
8000	$4.989 \cdot 10^{-4}$	1.977
9000	$3.953 \cdot 10^{-4}$	1.974
10000	$3.210 \cdot 10^{-4}$	1.975

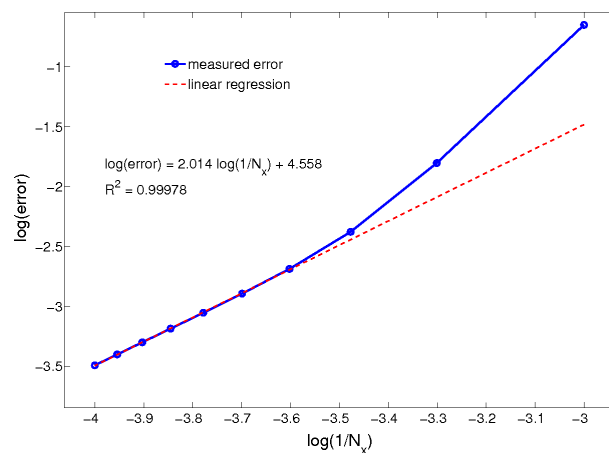


Figure 4: Test 1. Measure of convergence. Numerical error  $\varepsilon_n$  versus  $N_x$ .

### 5.3 Test 2: numerical validation of Biot-JKD

The aim of this test is to validate the mathematical and numerical modeling of the original Biot-JKD system. In figure 5, we compare the numerical Biot-AD (circle) and analytical Biot-JKD (solid line) values of the pressure, at  $t_1$  and  $t_2 > t_1$ . The parameters are given in section 5.2, in particular  $f_0 = 200$  kHz ( $f_0/f_c \approx 50$ ).

We observe the dispersion and the large attenuation of the slow wave. Excellent agreement between the two curves is obtained. More quantitatively, the relative error measured at  $t_1$  is  $\varepsilon_t \approx 1.95\%$ . The errors are due to the mathematical modeling (error of model  $\varepsilon_m$  between Biot-JKD and Biot-AD) and also to the numerical modeling (numerical error  $\varepsilon_n$  between exact and numerical values of Biot-AD). Thus the total error  $\varepsilon_t$  satisfies:

$$\varepsilon_t \leq \varepsilon_m + \varepsilon_n. \quad (21)$$

As seen in test 1,  $\varepsilon_n \approx 1.70\%$ . According to the figure 2, the choice  $N = 6$  leads to a relative error between the frequency correction functions  $\widehat{F}_{AD}(\omega)$  and  $\widehat{F}_{JKD}(\omega)$  (15) of 5.58%. The inequality (21) is therefore well satisfied.

## 6 Prospects

Various extensions of the present work are suggested:

- *2D algorithm.* Extension to 2D of the numerical methods is currently in progress. The validity of each numerical tools has already been established in 2D [6]. Parallelization of the algorithm will be performed also. To take in account the interfaces, an immersed interface method [6] will be implemented.
- *Thermal effects.* In the present work, the thermomechanical effects are neglected. To take them into account, we can consider the model of dynamic thermal permeability described in [4]. The formalism is analogous to the model of dynamic viscous permeability proposed by JKD, leading also to fractional derivatives of order  $1/2$ .
- *Heterogeneous medium.* In a homogeneous medium, we can compute the analytical solutions of Biot-JKD

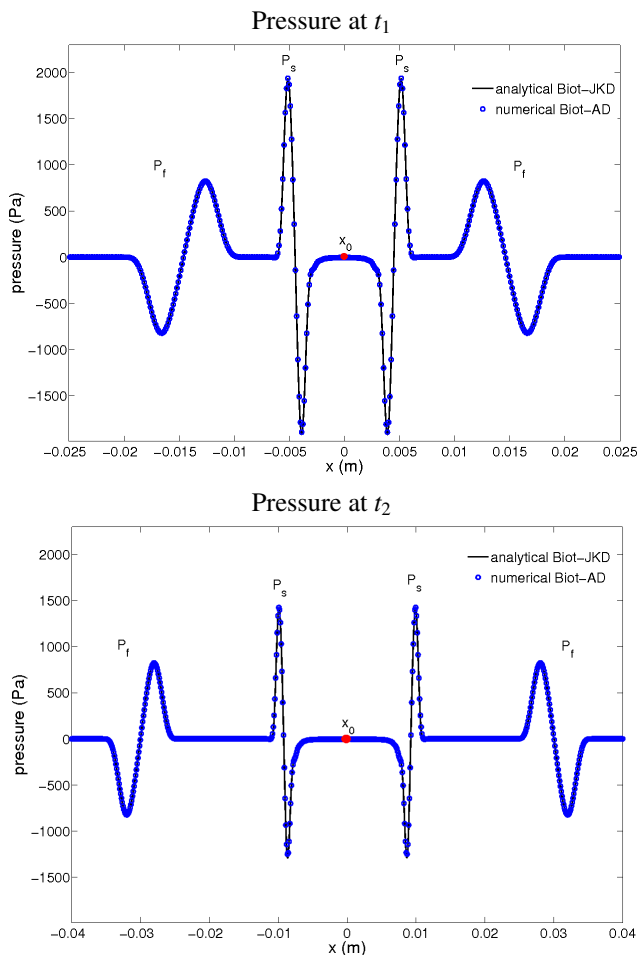


Figure 5: Test 1. Fast waves  $P_f$  and slow waves  $P_s$  generated by a point source centered on  $x_0 = 0$  m. Comparison between the numerical Biot-AD (circle) and analytical Biot-JKD (solid line) values of the pressure, with  $f_0 = 200$  kHz ( $f_0/f_c \approx 50$ ), at  $t_1 \approx 8.63 \cdot 10^{-6}$  s and  $t_2 \approx 1.51 \cdot 10^{-5}$  s.

model by Fourier synthesis, but it is out of reach when the Biot parameters of the medium vary continuously in space. On the contrary, the numerical tools presented along this paper are well-suited to this case.

## References

- [1] M.A. Biot, "Theory of propagation of elastic waves in a fluid-saturated porous solid. I: Low-frequency range", *J. Acoust. Soc. Am.*, **28**(2), 168-178 (1956).
- [2] M.A. Biot, "Theory of propagation of elastic waves in a fluid-saturated porous solid. II: High-frequency range", *J. Acoust. Soc. Am.*, **28**(2), 179-191 (1956).
- [3] D.L. Johnson, J. Koplik, R. Dashen, "Theory of dynamic permeability and tortuosity in fluid-saturated porous media", *J. Fluid Mech.*, **176**, 379-402 (1987).
- [4] D. Lafarge, P. Lemarinier, J.F. Allard, "Dynamic compressibility of air in porous structures at audible frequencies", *J. Acoust. Soc. Am.*, **102**(4), 1995-2005 (1997).
- [5] B. Lombard, J. Piraux, "Numerical modeling of transient two-dimensional viscoelastic waves", *J. Comput. Phys.*, **230**(15), 6099-6114 (2011).
- [6] G. Chiavassa, B. Lombard, "Time domain numerical modeling of wave propagation in 2D heterogeneous porous media", *J. Comput. Phys.*, **230**(13), 5288-5309 (2011).
- [7] E. Blanc, G. Chiavassa, B. Lombard, "Numerical modeling of 1D poroelastic waves with dissipative terms involving fractional derivatives", submitted to *J. Comput. Phys.* (2012).
- [8] F. Dubois, A. Galucio, N. Point, "Introduction à la dérivation fractionnaire : théorie et applications", <http://www.math.u-psud.fr/~fdubois>, (2010).
- [9] H. Haddar, J.R. Li, D. Matignon, "Efficient solution of a wave equation with fractional-order dissipative terms", *J. Comput. Appl. Math.*, **234**(6), 2003-2010 (2010).
- [10] J.F. Lu, A. Hanyga, "Wave field simulation for heterogeneous porous media with singular memory drag force", *J. Comput. Phys.*, **208**(2), 651-674 (2005).
- [11] H. Emmerich, M. Korn, "Incorporation of attenuation into time-domain computations of seismic wave fields", *Geophysics*, **52**(9), 1252-1264 (1987).
- [12] J.P. Groby, C. Tsogka, "A time domain method for modeling viscoacoustic wave propagation", *J. Comput. Acoust.*, **14**(2), 201-236 (2006).